

# **TIBIAL TORSION MEASUREMENT BY SURFACE CURVATURE**

Xiang Liu<sup>a</sup>, Wangdo Kim<sup>a</sup>, Burkhard Drerup<sup>b</sup>, Arjandas Mahadev<sup>c</sup>

<sup>a</sup>School of Mechanical and Production Engineering, Nanyang Technological University,  
Singapore

<sup>b</sup>Klinik und Poliklinik für Technische Orthopädie und Rehabilitation,  
Universtätsklinikum, Münster, Germany

<sup>c</sup>KK Hospital, Singapore

Correspondence Author:

Wangdo Kim

School of Mechanical and Production Engineering, Nanyang Technological University,  
50 Nanyang Avenue, Singapore 639798

Tel: (65) 67906890

Fax: (65) 67911859

Email: [mwdkim@ntu.edu.sg](mailto:mwdkim@ntu.edu.sg)

## Abstract

*Objective.* To measure the tibial torsion by curvature maps and study its reproducibility.

*Design.* In vivo lower leg surface registration on 6 pairs of legs of adult men.

*Background.* Tibial torsion is the angle between the transverse axes of the proximal and distal tibial articular surfaces, the degree of twisting of the tibia around its own longitudinal axis. The accurate measurement on the magnitude of tibial torsion is used when monitoring derangements in tibial torsion. It is also useful as a baseline in the event of surgical intervention. Various methods have been developed but none of them have gained wide acceptance. Even with the CT scan technique, the “gold standard” until now, has great variability in results amongst researchers. Thus an objective, non-invasive and fast method is needed for the monitoring of tibial torsion in the clinical environment.

*Methods.* The lower leg is scanned by a laser scanner, which gives the surface coordinates of the leg surface. By calculating the curvature maps of the leg from the 3D coordinates, stable anatomical landmarks such as the lateral and medial malleoli could be located. The angle indicating the degree of tibial torsion can then be derived from these landmarks together with the tibial condyles.

*Results.* The objective determination of the anatomical landmarks results in a reproducible determination of tibial torsion. The results obtained in this study are generally in agreement with the observed measurement reported previously.

*Conclusion.* The high reproducibility of the above method makes it suitable for measurement and monitoring the tibial torsion in the clinical setting.

**Relevance**

Tibial torsion determined by anatomical landmarks from curvature maps gives reproducible results, which allows tibial torsion to be observed, monitored and compared.

This will lead to a design of a measuring system, which is fast, convenient, accurate and free from radiation.

## 1. Introduction

Tibial torsion is the twisting of the tibia about its longitudinal axis, which changes as people grow up. Knowing the normal range of tibial torsion at different ages or tracking the changes is important for the monitoring of tibial torsion especially, if there are derangements. In order to reduce irreversible lower-limb rotational defects such as in-toeing and out-toeing in adults, the accurate determination of tibial torsion is necessary. Accurate measurement of tibial torsion also helps to study its relationship to the congenital clubfoot (Herold and Marcovich, 1976; Reikeras et al., 2001) and to the pathology of the knee such as patellofemoral instability or Osgood-Schlatter disease (Turner and Smillie, 1981).

Since it was first described by Le Damany (1903), tibial torsion has long been studied by various methods. The most accurate technique is measuring the angle formed by the pins passing through the transcondylar axis of the head of the tibia and the axis of the distal articular surface of the tibia but this method could not be used in vivo (Jakob et al., 1980). With the aid of mechanical apparatus such as caliper and goniometer, several simple and inexpensive methods have been used clinically. Staheli and Engel (1972) presented a simple clinical method by calculating the transmalleolar axis of 180 normal children and adults. With a C-clamp, Ritter et al. (1976) carried out a longitudinal examination on the tibiofibular rotation of the children at birth (1000 legs), 6 months (302 legs), 12 months (154 legs) and 24 months (105 legs). Malekafzali and Wood (1979) designed a simple

goniometric device, made up of one limb and two rubberized malleolar cups to measure the angle between the transcondylar and transmalleolar axes. Again, in 1985, Staheli et al. (1985) measured the angle between the line perpendicular to the transmalleolar axis and the thigh axis from the projected photographic negatives on 1000 lower limbs. Milner and Soames (1998) compared these four in vivo methods of measuring tibial torsion, aiming for a most accurate one. However, as the repeatability of the indirect techniques was low both in cadavers and the living, alternative clinical measurement methods of tibial torsion needed to be developed.

Besides the above researchers, many others tried different methods such as caliper (Wynne - Davies, 1964), tropometer (Herold and Marcovich, 1976), tractograph (Valmassy and Stanton, 1989), electronic digital inclinometer (Tamari and Tinley, 2003), roengenograph (Hutter and Scott, 1949; Rosen and Sandic, 1955; Herold and Marcovich, 1976), gravity goniometer (Lang and Volpe, 1998), computer topography (CT) (Jakob et al., 1980; Laasonen et al., 1984; Reikeras and Hoiseth, 1989; Kristiansen et al., 2001), magnetic resonance image (MRI) (Schneider et al., 1997), fluoroscopy (Clementz and Magnusson, 1989) and ultrasound (US) (Butler-Manuel et al., 1992). Each method has its own advantage and disadvantage. The simple clinical assessment depends largely on the examiner's preference and experience. Roentgenographic methods require trained personnel, present additional radiological expense and exposure and when applied to children, incomplete ossification makes interpretation difficult. Some final assessing tibial torsion using radiographs of the tibia is unhelpful (Li and Leong, 1999). The position of the subjects' leg and the different plane of the cut will introduce artifacts to

the CT assessment. Laasonen et al. (1984) doubted the clinical use of CT because of its wide variation. As a possible alternative of CT, measurements by MRI will also vary according to the plane of the image. Fluoroscopy requires a stable knee joint as a prerequisite. US can only obtain full cross sectional images of tibia with much difficulty. As such, a new method, different from Jend's established CT method (Jend et al., 1981) and by Butler-Manuel (Butler-Manuel et al., 1992), has to be developed to measure tibial torsion.

The two reference lines that give the angle of tibial torsion also differ with different references. Many researchers took the transmalleolar axis as the distal reference line. For the proximal reference line, some researchers turned to the tibial tubercle when they measured tibial torsion (Wynne - Davies, 1964) or when they tried to reproduce others' experiments for comparison purpose (Herold and Marcovich, 1976; Lang and Volpe, 1998). However, in the viewpoint of Lang and Volpe (1998), using the tibial tubercle as a proximal reference point might not give a true measurement of tibial or tibiofibular torsion. Some other researchers took the dorsal tangent to the tibial condyles (Laasonen et al., 1984; Butler-Manuel et al., 1992; Schneider et al., 1997) or the dorsal tangent to the femur condyles (Kristiansen et al., 2001). Whereas Reikeras and Hoiseth (1989) found that the anatomy of the dorsal aspects of the femoral condyles gave more stable results than those of the tibial condyles. However, this might only be true for healthy subjects. Jend et al. (1981) pointed out that by using dorsal condylar contour of the femur, errors are likely due to the axial rotation of the knee if the knee could not be straightened due to trauma or if excessive laxity exists.

Different researchers measure this angle with different methods and reference lines, resulting in a huge variation in the reported normal ranges of tibial torsion. Each method has its own advantages and disadvantages and no conventional technique for routine assessment of tibial torsion has gained wide acceptance yet.

Measurement by simple apparatus, although convenient and inexpensive, is inaccurate due to subjectivity. The ideal means of quantification of tibial torsion should be simple, rapid, inexpensive, reliable and suitable for a busy clinical environment and minimize subjective variables (Malekafzali and Wood, 1979). Thus a new method which satisfies the above requirements and at the same time eliminates the subjectivity is needed.

In the authors' previous works (Liu et al., 2004), a method for extraction of curvatures and evaluation of prominent features on foot and lower leg surface was developed. The goal was to attain approximate surfaces to the unevenly distributed data measured by the 3D non-contact scanner. By checking curvature maps the landmarks were characterized and discriminated. In this way, tibial torsion can be measured by surface curvature. Scanning the lower leg and extracting anatomical landmarks to calculate the angle provides an objective way of measuring tibial torsion compared to other methods, which are subjected to examiner's experience and preference (Elftman, 1945; Ritter et al., 1976; Milner and Soames, 1998). In this paper, a basic technical description of the method and

its application in a pilot study are presented, promising to provide a fast, convenient and accurate way free from radiation, cost and subjective disturbance to measure tibial torsion. The reproducibility of the method was also evaluated.

## 2. Methods

### *2.1 Experimental procedure*

Measurement was done by the FastSCAN Scanner (Polhemus, Colchester, Vermont, USA). FastSCAN is a fast and convenient way to scan the object's surface and provides 3D coordinates for the surface points. The measurement is done by handling the FastSCAN Magic Wand to sweep slowly and smoothly over the surface just as one sprays painting on it. The Magic Wand consists of a centrally mounted diode line laser generator and two miniature cameras. The laser is cast on the surface and the intersection is viewed by the two cameras from two different directions. A tracker operates a transmitter and two receivers to calculate the position and orientation of the Magic Wand which allows the computer to reconstruct the surface. The three-dimensional image can be displayed simultaneously on the computer screen. The data can be transformed and exported with various file types.

Six subjects were tested and informed consent was obtained from each of the subjects before scanning. The subjects are healthy and no one has a history of lower extremity surgery. When their legs were scanned, subjects sat comfortably on a chair with their legs

in the neutral position, bent 90 degree to the thigh. During the scanning, they tried their best to stay stationary. One receiver was attached to the shank so that it moved with the leg in order to minimize the influence of involuntary movement. In our scanning several views from different directions were taken. For the complete measurement of the whole lower leg, the individual views were merged into a single file. The data was then saved in the form of text files for further process. The density of measurement points was about 40 points/cm<sup>2</sup>. The scanning time is less than one minute and processing time is less than 5 minutes. This could be further reduced at the expense of image resolution.

## *2.2 Surface fitting*

A plain understanding of shape characteristics leads to a classification into plane and curved surfaces. Cylinders are curved in one direction only – they are called surfaces of revolution or parabolic surfaces. If a surface is curved in two orthogonal directions it may be concave, convex or saddle-shaped. Concave or convex surfaces are called elliptic and saddle-shaped surfaces are called hyperbolic.

The sign of the Gaussian curvature enables elliptic areas to be distinguished from hyperbolic areas. Similarly in the case of parabolic and elliptic areas, one can easily distinguish convexity from concavity by the sign of mean curvature (Frobin and Hierholzer, 1982). It is easy to calculate the Gaussian curvature and mean curvature once the analytical description of the surface has been given. But from the experiment, we can only get discrete data, for example, the (x, y, z) coordinates of isolated points. On the

other hand, a parametrized representation of the surface based on a regular coordinate grid implies a great simplification in different aspects: standardization in the calculation and representation of curvatures, and an easier comparison of surfaces. To extract a grid point from the scattered data, we need to consider fitting a small second order polynomial surface patch to the points neighbouring the grid points. A set of regular grid points has the following form:  $x_{ik} = g \cdot i$ ,  $y_{ik} = g \cdot k$ ,  $z_{ik} = f(x_{ik}, y_{ik})$ , where  $i$  and  $k$  are grid indices and  $g$  is the grid constant. We can transform our randomly distributed data into such regular grid data by introducing a second order polynomial patch with six degrees of freedom:

$$z = c_1 + c_2p + c_3q + c_4p^2 + c_5pq + c_6q^2 \quad (1)$$

where  $c_1$  to  $c_6$  are the unknown coefficients,  $p$  and  $q$  are the local coordinates with respect to the respective grid point  $(x_{ik}, y_{ik})$  centring the fitted patch:

$$p = x - x_{ik}, \quad q = y - y_{ik} \quad (2)$$

Scanned surface data provides a set of points for each patch in the form of  $(x_i, y_i, z_i)$ , where  $i$  varies from 1 to  $n$  and  $n$  is the number of measured data points within a patch. Fitting the patch is carried out by the least squares condition. For each data point in the patch, we have the measured  $z$  ( $z_i$ ) and the calculated  $z$  ( $z_i'$ ) from equation (1).

$$\begin{Bmatrix} z_1' \\ z_2' \\ \mathbf{M} \\ z_i' \\ \mathbf{M} \\ z_n' \end{Bmatrix} = \begin{bmatrix} 1 & p_1 & q_1 & p_1^2 & p_1q_1 & q_1^2 \\ 1 & p_2 & q_2 & p_2^2 & p_2q_2 & q_2^2 \\ \mathbf{M} & \mathbf{M} & \mathbf{M} & \mathbf{M} & \mathbf{M} & \mathbf{M} \\ 1 & p_i & q_i & p_i^2 & p_iq_i & q_i^2 \\ \mathbf{M} & \mathbf{M} & \mathbf{M} & \mathbf{M} & \mathbf{M} & \mathbf{M} \\ 1 & p_n & q_n & p_n^2 & p_nq_n & q_n^2 \end{bmatrix} \begin{Bmatrix} c_1 \\ c_2 \\ c_3 \\ c_4 \\ c_5 \\ c_6 \end{Bmatrix} \quad (3)$$

We aim to get the coefficients  $c_1, c_2, c_3, c_4, c_5$  and  $c_6$  in such a way that the discrepancy  $z'_i - z_i$  between the fitting surface patch and the measurement data points should be minimized. We find  $z'_i$  by choosing the coefficients  $c_1 \dots c_6$  to minimize the sum of squared differences,  $E(z)$ :

$$E(z) = \sum_{i=1}^n (z'_i - z_i)^2 = \sum_{i=1}^n (z(p_i, q_i) - z_i)^2 \quad (4)$$

A weighting function is used to put weightings on the data points with respect to their distances to the grid point (the centre point). The weightings drop off with increasing distance from the centre point thus the weightings of the points are not equal over the whole area. We introduce a diagonal weighting matrix  $\mathbf{G}$  to meet the requirement.

$$\mathbf{G} = \text{Diag}(g_1, g_2, \dots, g_n) \quad (5)$$

$$g_i = f \cdot (\exp(-(p_i^2 + q_i^2)/d^2)) \quad i=1, 2, \dots, n \quad (6)$$

where  $d$  is the grid spacing constant, and  $f$  is the factor adjusted with respect to the point's distance to the centre point.

With the weighting incorporated equation (4) becomes

$$E(z) = \sum_{i=1}^n g_i (z(p_i, q_i) - z_i)^2 \quad (7)$$

The function  $E$  of  $c_1, c_2, c_3, c_4, c_5$  and  $c_6$  will have a minimum only when

$$\partial E / \partial c_i = 0, \text{ for } i=1, 2, \dots, 6. \quad (8)$$

These conditions yield six linear equations in the unknowns  $c_1, c_2, c_3, c_4, c_5$  and  $c_6$ .

Solving these six linear equations, we can get the six coefficients  $c_1, c_2, c_3, c_4, c_5$  and  $c_6$ .

Thus, we fit the second order polynomial surface patch in a small area around the centre point by the least squares method. At the same time the irregular data points have been transformed into points on the intersections of grid. The first component of  $\mathbf{C}$ ,  $c_1$ , is the  $z$  coordinate of the grid point. The other components ( $c_2, c_3, c_4, c_5$  and  $c_6$ ) can be interpreted as the coefficients  $x_p, x_q$  etc. which are the first and second derivatives of  $x$  with respect to  $p, q$  at a surface point  $(x_{ik}, y_{ik}, z_{ik})$ . As described in (Frobin and Hierholzer, 1982), from the coefficients the principal curvatures, mean curvature, Gaussian curvature and Koenderink shape index (Koenderink and van Doorn, 1992) can be calculated. The operator then moves along by one grid constant to the next centre point until the whole measured surface is covered. To separate convexity from concavity, the map of Koenderink shape index is drawn.

The Koenderink shape index map of the lower leg (Fig. 1) shows several anatomical landmarks that are mainly formed by the bone underlying the skin. Two lines are defined by the conspicuous anatomical landmarks: the two malleoli, the fibular head, the point anterior to lateral tibial condyle and the medial tibial condyle. The angle between the two lines is taken as a measurement of tibial torsion. In 3D space, if line 1 is decided by two

points  $\mathbf{x}_1$  and  $\mathbf{x}_2$  and line 2 by  $\mathbf{x}_3$  and  $\mathbf{x}_4$  (Fig. 2), then the angle  $\theta$  between the two lines is calculated as

$$\cos \theta = \frac{(\mathbf{x}_2 - \mathbf{x}_1) \bullet (\mathbf{x}_4 - \mathbf{x}_3)}{|\mathbf{x}_2 - \mathbf{x}_1| |\mathbf{x}_4 - \mathbf{x}_3|} \quad (9)$$

### *2.3 Reproducibility of localization of anatomical landmarks and tibial torsion measurement*

In our experiment, the landmarks are defined by the centre of gravity  $(\frac{\sum_{i=1}^N x_i}{N}, \frac{\sum_{i=1}^N y_i}{N}, \frac{\sum_{i=1}^N z_i}{N})$  of those N points with Koenderink shape index larger than a certain threshold. To study the reproducibility of localization of anatomical landmarks, a 26-year-old healthy man's right foot was scanned at the ankle area when he sat comfortably on the chair. The distance between the outer and inner malleoli was calculated. Three different examiners scanned the man's right foot on three consecutive days. Each examiner scanned the malleoli eight times. The ANOVA is used to check whether there is any significant difference between the means of different groups.

The reproducibility of tibial torsion measurement is investigated from the scanning on two male's right legs by three different examiners on three consecutive days, eight scanning on each man's right leg. The ANOVA is used again to detect whether there is any significant difference on the right leg's tibial torsion scanned by different examiners.

### 3. Results

The bimalleolar distance measured by three different testers (Fig. 3) gave almost the same mean of different measurement with small standard deviation. The results of ANOVA ( $p=0.89$ ) indicate good reproducibility of the localization of the landmarks by finding the centre of gravity of points. Certainly, the number of points (N) chosen has an influence on the final location of the landmarks. But as the number (N) is large enough, this influence is minimized as well as the noise effect on the shifting of the final location. For comparison, the number of points selected for calculating the centre of gravity should be consistent among subjects with the precondition that these points cover the area of interest. The number (N) varies with point density for the same region of interest. With our scanning, we find that 40 is the ideal number.

The reproducibility of this definition was good, judging from the results of ANOVA (Fig. 4,  $p=0.74$  and  $p=0.80$  for subject 1 and 2 respectively). The angle of tibial torsion determined by the two lines had a relatively large variance with contributions from all the errors caused by localizing the five anatomical landmarks. Still, no significant difference was found among the means of the results from different testers on subject 1 and 2. Scanning the leg and determining the anatomical landmarks from the curvature maps gave an objective and reproducible way of measuring tibial torsion.

Three pairs of legs from adult males were scanned, and the tibial torsion measurement ranged from  $15.95^\circ$  to  $26.98^\circ$ , indicating a wide variation in tibial torsion even among

normal subjects. This range, however, is in concurrence with the normal values of tibial torsion being from 0 to 45° with a mean of 25° (Staheli et al., 1985). Looking at Table 1, we found a difference between left and right tibial torsions with the right being greater. This was supported by other researchers (Butler-Manuel et al., 1992; Schneider et al., 1997). However, on the contrary, other researchers claimed that no significant difference was found between the sides (Jakob et al., 1980; Reikeras and Hoiseth, 1989; Valmassy and Stanton, 1989; Stuberg et al., 1991). The small sample size and the use of only 3 pairs of legs limit the generalization of the findings. More subjects are required in order to study the difference between left and right tibiae.

## 4. Discussion

The main problem of various techniques employed by different researchers is the subjective nature of the methods chosen. This seems unavoidable due to the lack of suitable landmarks on the leg (Milner and Soames, 1998). Tibial torsion is measured by the angular relationship of a line drawn between two points in the proximal ends of the bones with a line drawn between two points in the distal ends of the bone. Therefore four fixed points need to be determined. Although choice of the two pairs of points is arbitrary, they must be constant (Rosen and Sandic, 1955). The method presented here has characterized the lower leg and objectively provided several stable anatomical landmarks to be used for the measurement of tibial torsion. The previously inconsistent localization of the malleoli by palpation, which resulted in subjective and inaccurate measurement, is replaced by the objective determination of their position on the curvature maps. The anatomical landmarks selected as reference points are constant from bone to bone and study to study. This ensures high reproducibility of the tibial torsion measurement. As such, accurate comparisons can be made.

This proposed method however is not as accurate as the measurements obtained by CT and MRI since it does not obtain the measurement from the bone. The motion between tibia and fibula will introduce errors (the tibiofibular torsion is about  $5^\circ$  less than actual tibial torsion (Valmassy and Stanton, 1989)). This cannot be avoided but can be minimized by studying on the range of tibia-fibular motion (Khermosh et al., 1971). However, as long as the technique produces reproducible angles, a consistent relationship

to the direct measurement is ensured. This will allow for the calculation of the true tibial torsion based on this relationship. Future work can be carried out to determine the relationship between this method and direct measurement on the tibial bone itself.

Scanning the whole leg is unnecessary. In a busy clinic environment, only the areas relevant in the determination of tibial torsion are scanned. They are the area below the knee and the medial and lateral malleoli. This results in a shorter time used for scanning. The scanned surfaces can be stored in a database so that the changes of the tibial torsion could be monitored during follow up and mapped. This is especially useful in children that require rotational osteotomies in case of abnormal tibial torsion, which does not correct after regular monitoring of the tibial torsion. It can also be used to determine objectively the post-operation correction.

This method does not work on the obese subjects as the anatomical landmarks are not distinguishable from the surrounding subcutaneous fat. The solution to this problem might then be to look for other anatomical landmarks that are more obvious in these obese subjects such as the tibial tuberosity or the medial surface of the tibia (Tamari and Tinley, 2003). Then the angle can be calculated differently and the relationship with the CT and MRI measurements adjusted accordingly.

## 5. Conclusion

This paper investigates the feasibility of objective measurement of tibial torsion in 6 subjects. The objective determination of anatomical landmarks used for measuring tibial torsion results in the high reproducibility of the measurement. The method could become a fast, objective and non-invasive way at least for screening purpose if its reproducibility and accuracy are further verified in vitro by the most accurate method of pins passing through the articular surface of tibia on necropsy specimen or in vivo by CT involving a large number of subjects.

Figure 1: The reconstructed surface (left) and the Koenderink shape index map (right) of the lower leg (Red: convex, green: saddle-shaped, blue: concave, white: transitions between these three different shapes.). Five anatomical landmarks (\*) are localized to form the proximal and distal reference lines. A: the fibular head. B: the anterior aspect of the lateral tibial condyle. C: The medial tibial condyle. D: outer malleolus. E: inner malleolus. The proximal reference line connects the mid point of A and B with C. The distal reference line is the transmalleolar axis. The angle between these two reference lines is calculated as tibial torsion.

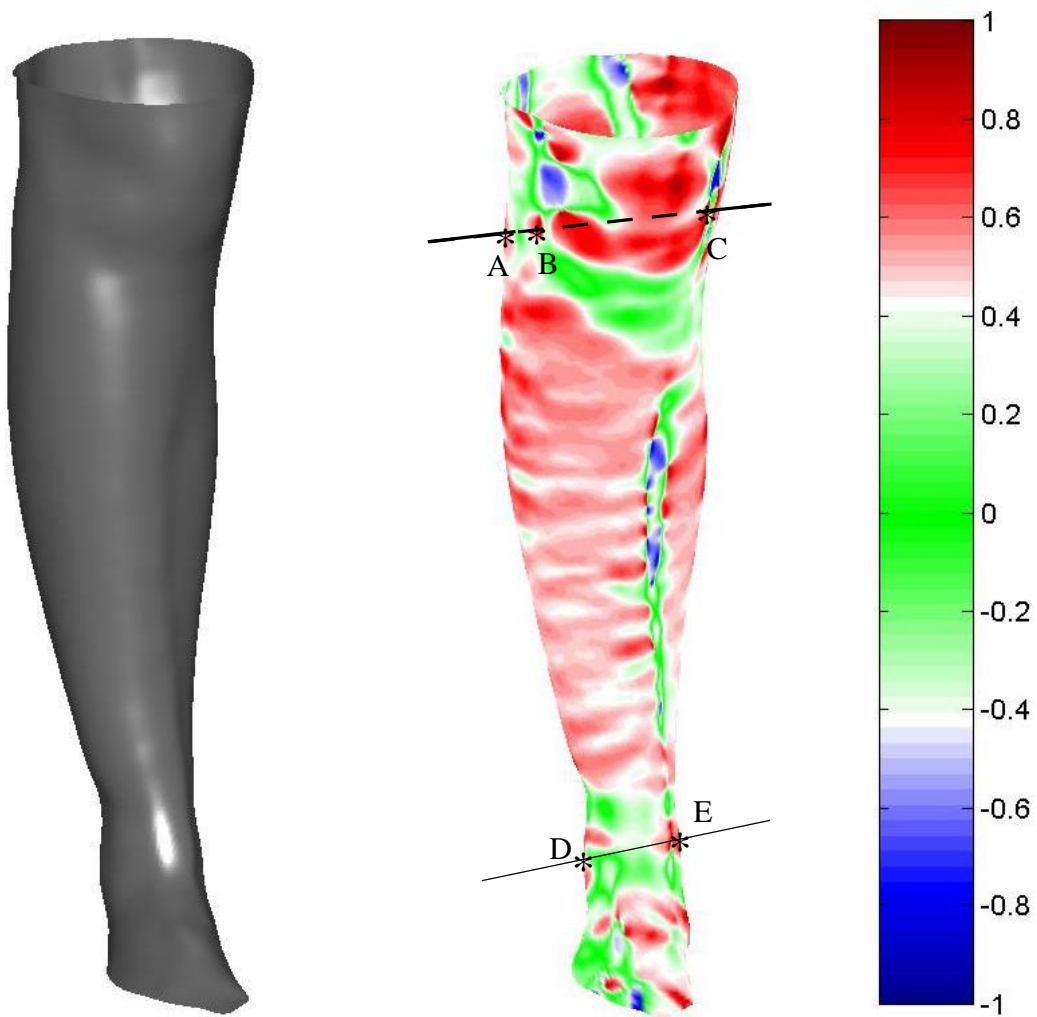


Figure 2: The angle between two lines in 3d space.

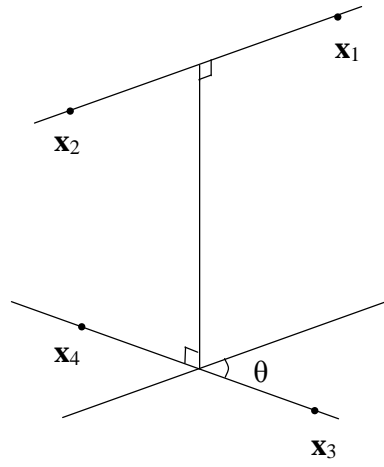


Figure 3: The box plot of the bimalleolar distance measured by three different testers.

The box has lines at lower quartile, median and upper quartile values. The lines extending from each end of the box show the extent of the rest of the data.

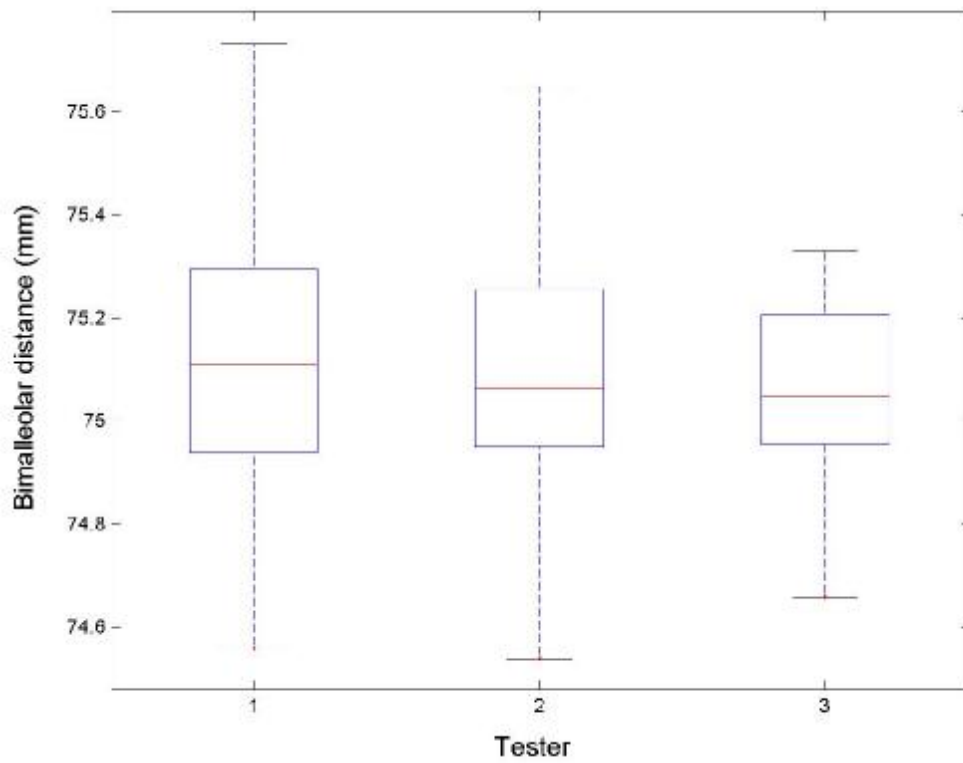


Figure 4: The box plot of tibial torsion measured by three different testers on two subjects' right legs. The box has lines at lower quartile, median and upper quartile values. The lines extending from each end of the box show the extent of the rest of the data. No significant difference is found among the means of results from different testers on subject 1 (left) and 2 (right).

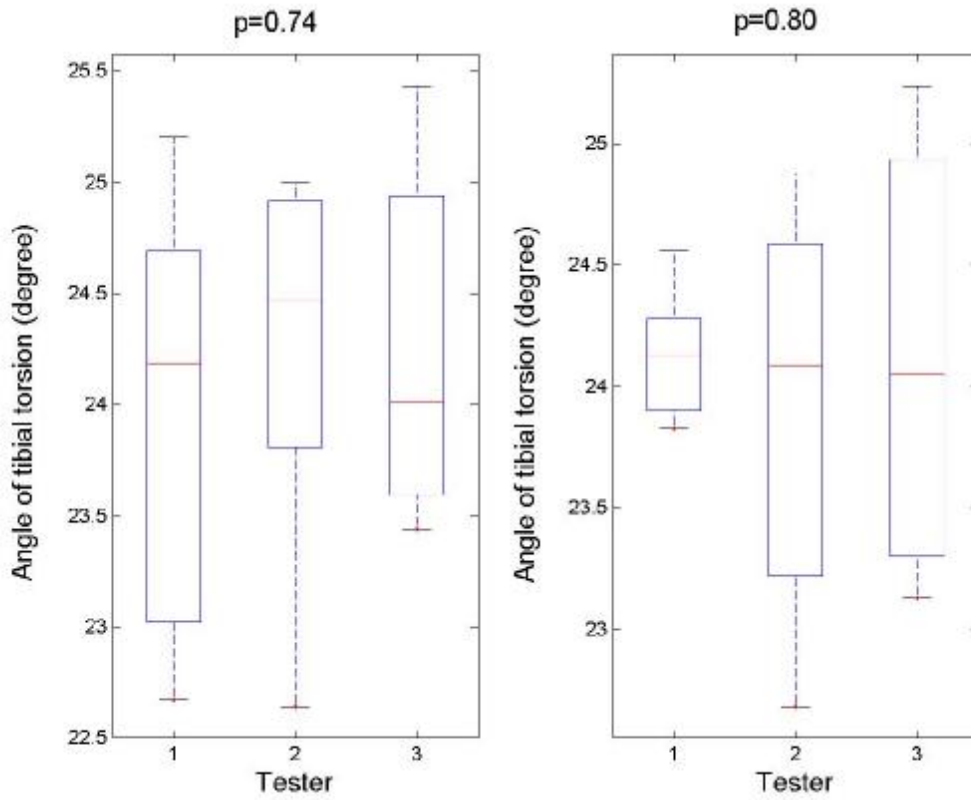


Table 1: The tibial torsion of the 6 subjects. All legs are scanned once except subject 5 and 6's right legs for reproducibility study, whose mean and standard deviation are calculated from the 24 scans.

Subjects	Left	Right
1	20.57	21.77
2	19.52	22.98
3	26.90	26.98
4	15.95	16.38
5	23.77	24.05±0.70
6	20.86	24.15±0.84

## Reference

- Butler-Manuel, P., Guy, R., Heatley, F., 1992. Measurement of tibial torsion--a new technique applicable to ultrasound and computed tomography. *The British Journal of Radiology* 65, 119-126.
- Clementz, B., Magnusson, A., 1989. Assessment of tibial torsion employing fluoroscopy, computed tomography and the cryosectioning technique. *Acta Radiologica (Stockholm, Sweden : 1987)* 30, 75-80.
- Elftman, H., 1945. Torsion of the lower extremity. *American Journal of Physical Anthropology* 33, 255-265.
- Frobin, W., Hierholzer, E., 1982. Analysis of human back shape using surface curvatures. *Journal of Biomechanics* 15, 379-390.
- Herold, H.Z., Marcovich, C., 1976. Tibial torsion in untreated congenital clubfoot. *Acta Orthopaedica Scandinavica* 47, 112-117.
- Hutter, C.G., Scott, W., 1949. Tibial torsion. *The Journal of Bone and Joint Surgery. American Volume* 31, 511-518.
- Jakob, R.P., Haertel, M., Stüssi, E., 1980. Tibial torsion calculated by computerised tomography and compared to other methods of measurement. *The Journal of Bone and Joint Surgery* 62-B, 238-242.
- Jend, H., Heller, M., Dallek, M., Schoettle, H., 1981. Measurement of tibial torsion by computer tomography. *Acta Radiologica: Diagnosis* 22, 271-276.
- Khermosh, O., Lior, G., Weissman, S., 1971. Tibial torsion in children. *Clinical Orthopaedics and Related Research* 79, 25-31.

- Koenderink, J., van Doorn, A., 1992. Surface shape and curvature scales. *Image and Vision Computing* 10, 557-565.
- Kristiansen, L., Gunderson, R., Steen, H., Reikeras, O., 2001. The normal development of tibial torsion. *Skeletal Radiology* 30, 519-522.
- Laasonen, E.M., Jokio, P., Lindholm, T.S., 1984. Tibial torsion measured by computed tomography. *Acta Radiologica: Diagnosis* 25, 325-329.
- Lang, L.M.G., Volpe, R.G., 1998. Measurement of tibial torsion. *Journal of the American Podiatric Medical Association* 88, 160-165.
- Le Damany, P., 1903. Technique of tibial tropometry (translated). *Clinical Orthopaedics and Related Research* 302, 4-10.
- Li, Y.H., Leong, J.C., 1999. Intoeing gait in children. *Hong Kong Medical Journal* 5, 360-366.
- Liu, X., Kim, W., Drerup, B., 2004. 3D characterization and localization of anatomical landmarks of the foot by fastscan. *Real-Time Imaging* In print.
- Malekafzali, S., Wood, M.B., 1979. Tibial torsion - A simple clinical apparatus for its measurement and its application to a normal adult population. *Clinical Orthopaedics and Related Research* 145, 154-157.
- Milner, C.E., Soames, R.W., 1998. A comparison of four in vivo methods of measuring tibial torsion. *Journal of Anatomy* 193, 139-144.
- Reikeras, O., Hoiseth, A., 1989. Torsion of the leg determined by computed tomography. *Acta Orthopaedica Scandinavica* 60, 330-333.

Reikeras, O., Pal Kristiansen, L., Gunderson, R., Steen, H., 2001. Reduced tibial torsion in congenital clubfoot: CT measurements in 24 patients. *Acta Ophthalmologica Scandinavica* 72, 53-56.

Ritter, M.A., DeRosa, G.P., Babcock, J.L., 1976. Tibial torsion? *Clinical Orthopaedics and Related Research* 00, 159-163.

Rosen, H., Sandic, H., 1955. The measurement of tibiofibular torsion. *The Journal of Bone and Joint Surgery. American Volume* 37, 847-855.

Schneider, B., Laubenberger, J., Jemlich, S., Groene, K., Weber, H.M., Langer, M., 1997. Measurement of femoral antetorsion and tibial torsion by magnetic resonance imaging. *The British Journal Of Radiology* 70, 575-579.

Staheli, L.T., Corbett, M., Wyss, C., King, H., 1985. Lower-extremity rotational problems in children. Normal values to guide management. *The Journal of Bone and Joint Surgery. American Volume* 67, 39-47.

Staheli, L.T., Engel, G.M., 1972. Tibial torsion: a method of assessment and a survey of normal children. *Clinical Orthopaedics and Related Research* 86, 183-186.

Stuberg, W., Temme, J., Kaplan, P., Clarke, A., Fuchs, R., 1991. Measurement of tibial torsion and thigh-foot angle using goniometry and computed tomography. *Clinical Orthopaedics and Related Research* 208-212.

Tamari, K., Tinley, P., 2003. A new concept of estimating tibiofibular torsion: an in vivo reliability study. *The Journal of Orthopaedic And Sports Physical Therapy* 33, 85-90.

Turner, M.S., Smillie, I.C., 1981. The effect of tibial torsion on the pathology of the knee. *The Journal of Bone and Joint Surgery. British Volume* 63-B, 396-398.

Valmassy, R., Stanton, B., 1989. Tibial torsion. Normal values in children. *Journal of the American Podiatric Medical Association* 79, 432-435.

Wynne - Davies, R., 1964. Talipes Equinovarus. A review of eighty-four cases after completion of treatment. *Journal of Bone and Joint Surgery* 46 B, 464 - 476.